POLITECNICO DI TORINO
Repository ISTITUZIONALE

Numerical modelling of the mechanical response of lattice structures produced through AM

(Article begins on next page)

08 November 2022

IGF26 - 26th International Conference on Fracture and Structural Integrity

Numerical modelling of the mechanical response of lattice structures produced through AM

M. Della Ripa[a], D.S. Paolino[a], A. Amorese[b], A. Tridello[a]*

[a]Politecnico di Torino, Department of Mechanical and Aerospace Engineering, Corso Duca degli Abruzzi 24, 10129 Turin, Italy
[b]Altair Engineering S.r.l, Via Livorno 60, 10144, Turin, Italy

Abstract

In the last years, with the development of Additive Manufacturing processes, the research on the mechanical behaviour of lattice structures has gained significant attention. Depending on the application, the mechanical properties of the unit cell can be modified by varying its geometry. The cell geometry is generally designed through Finite Element Analyses. However, the simulation of the mechanical response of components made of lattice structures can be rather complex, due to the long computation time. Therefore, efficient simplified models should be employed, but, in this case, an experimental validation is required.

In the paper, experimental compression tests are carried out on cubic specimens in lattice structures produced with a carbon nylon filament through a Fused Deposition Modeling process and with an AlSi10Mg alloy through a Selective Laser Melting process. The tests on carbon nylon specimens are carried out to assess the cell geometry ensuring the highest energy absorption among five selected cell geometries. Subsequently, a Finite Element (FE) model of the lattice structure specimens is created by using 1D beam elements and experimentally validated with the results obtained by testing manufactured specimens. The activity in the paper proves the effectiveness of models with 1D elements for the simulation of the mechanical response of the lattice structures and the importance of validating FE models to assess their real failure mode.

* Corresponding author. Tel.: +39 011 0906913;
  E-mail address: andrea.tridello@polito.it

1. Introduction

In the last years, with the development of Additive Manufacturing (AM) processes, the research on the mechanical behaviour of lattice structures has gained significant attention among researchers working at university and in industry. Lattice structures are three-dimensional structures composed of topologically ordered open cells and obtained through the repetition of a unit cell. The unit cell is composed of struts that are connected at nodes [1]. By modifying the geometry and the characteristic dimensions (e.g., the strut size) of the unit cell, the mechanical properties of the component made of lattice structures can be optimized, depending on the application. Lattice structures are generally produced with AM technology, which permits the manufacturing of their complex shapes, hardly producible with traditional manufacturing processes. Moreover, AM enables to integrate lattice structures within the component, limiting its weight without affecting its mechanical properties [2]. Lattice structures are exploited in several fields, e.g., for biomedical applications [3], for heat exchanger [4] or for energy absorption [5], [6], with a cell geometry that must be properly designed, depending on the application. The cell geometry and the final component are generally designed through Finite Element Analyses (FEAs) [[7],[8], [9]. However, the simulation of the mechanical response of components made of lattice structures can be rather complex and long, due to the small size of the struts with respect to the component size. To reduce the computational time, efficient simplified models can be employed, but, in this case, an experimental validation is required.

In the paper the mechanical response of specimens made of lattice structures and produced with AM technologies is experimentally and numerically assessed. The main objective is to define the cell geometry that can be used for the design of components in lattice structures for energy absorption applications and to develop efficient FEAs for the simulation of their response.

In particular, experimental compression tests are carried out on cubic specimens in lattice structures produced with a carbon nylon filament and a Fused Deposition Modeling (FDM) process and on cubic specimens in lattice structures produced in AlSi10Mg alloy with a Selective Laser Melting (SLM) process. The tests on carbon nylon specimens are performed to assess the cell geometry ensuring the highest energy absorption among five selected cell geometries. Subsequently, tests on AlSi10Mg specimens with the optimal cell geometry are carried out. A simplified model with 1D beam elements is also created to simulate the compression tests. The model has been validated on the experimental results obtained by testing the carbon nylon and the AlSi10Mg alloy specimens.

The results in this paper highlight the importance of experimentally validating finite element models for the simulation of parts made of lattice structures and provide an experimental/numerical methodology for the design of lattice structures, to be used in components in-service conditions.

Nomenclature

AM	Additive Manufacturing
FEA	Finite Element analysis
FDM	Fused Deposition Modeling
SEA	Specific Absorbed Energy
SLM	Selective Laser Melting

---

2. Experimental activity description

In this Section, the experimental activity and the testing configuration are described. In Section 2.1, the geometries of the cell experimentally tested are described. In Section 2.2, the properties of the materials used for the experimental tests are reported. In Section 2.3, the testing configuration for compression tests is described.

2.1. Cell geometries

In the literature, many cell geometries have been proposed and analyzed [10,11]; in particular, the geometries of the unit cell are analytically defined and then verified through FEAs [11]. In the present work, the cell ensuring the highest energy absorption is experimentally assessed through compression tests. In particular, the compression tests are carried out on specimens made of carbon nylon ad printed with the FDM technology. It is worth noting that this material may not be the material used for the production of a component for energy absorption applications, but this analysis provides in any case useful indications on the absorption capability of a specific cell.

Five specimen geometries are tested: they have been selected from the most used in the literature and from a numerical study carried out in Altair. The file used for the specimen production with the FDM technology is created by using the software CREO 3D. The unit cells considered in this preliminary analysis are reported in Figure 1, together with the nomenclature adopted.
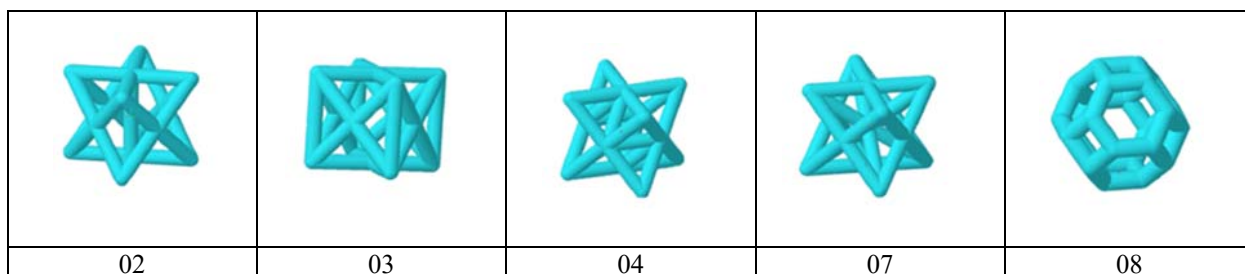

| 02 | 03 | 04 | 07 | 08 |

Fig. 1. Geometries of the unit cell tested in the present paper.

In [11], ten lattice geometries produced through SLM technology in AlSi10Mg have been analyzed. From the analysis of the literature results, the "octet" cell, 04, has been firstly selected. This is one of the most used cell geometry in the literature. Starting from this cell, cells 02 and 07 have been designed, and they differ from the original 04-01 for their internal structure. Cell 03, on the other hand, has been designed by eliminating in cell 04 the internal beam and inserting vertical beams at the four edges. The last investigated cell, 08, has been chosen, among the cells that can be inscribed in a cube, for its low reticular density [10].

The specimen geometry has been defined according to [12]. In [12], experimental tests have been carried on specimens with an increasing number of cells, one to seven, with step of two. For the specimens with three cells, a layer-by layer damage is observed, whereas for specimens with more than three cells a 45° degrees initial progressive damage and a following mixed compressive-shear damage has been experimentally found, thus not permitting to properly assess the compression behaviour of the investigated cell. According to the above-described analysis, cubic specimens with 3x3 cells (3x3 cells on the base and 3 cells along the height, according to Fig. 2) have been created, with the following characteristics:

- Strut diameter: 1.5 mm.
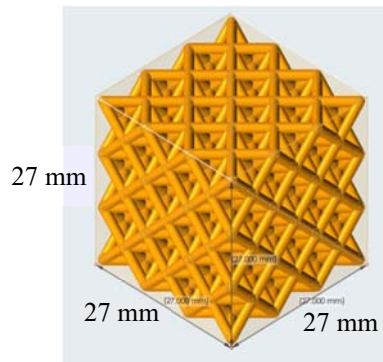- Length of the cubic cell side: 9 mm

Fig. 2. 3D model of a cubic cell specimen used for the experimental tests (cell 04).

It is worth noting that the cubic cell characteristics have been defined by considering also the production processes (FDM and SLM) used for the production of the specimens. If different production processes and materials are used, the selected characteristics, e.g., the strut diameter, may be changed. Sensitivity analyses on the influence of the cell characteristics should be carried out to assess the interaction between the cell properties and the material/production process considered.

2.2. Material properties and production

Cubic specimens are produced with an Ultimaker 5s FDM printer equipped with an Olsson Ruby nozzle and by considering the process parameters suggested by the filament supplier. The filament used for the production is a Fabbrix® nylon carbon filament with 2.85 mm diameter [13]. Two specimens are produced for each of the five cell types (Fig. 1).

Two specimens with the cell ensuring the highest energy absorption capability are then manufactured through SLM with an AlSi10Mg alloy, typically adopted for crashworthiness applications. The specimens are manufactured and heat-treated by BeamIt (Fornovo di Taro, Italy). Process parameters and post-process heat treatment have been set by the manufacturer.

2.3. Testing configuration

Compression tests are performed with a Zwick-Roell Z100 testing machine, at a constant crosshead speed of 1 mm/minute. The compression tests are also recorded with a Dino-Lite microscope placed near the specimens in order to assess the failure mode. Fig. 3 shows the testing setup for the compression tests and an example of the image acquired by the Dino Lite Microscope placed near the specimen.
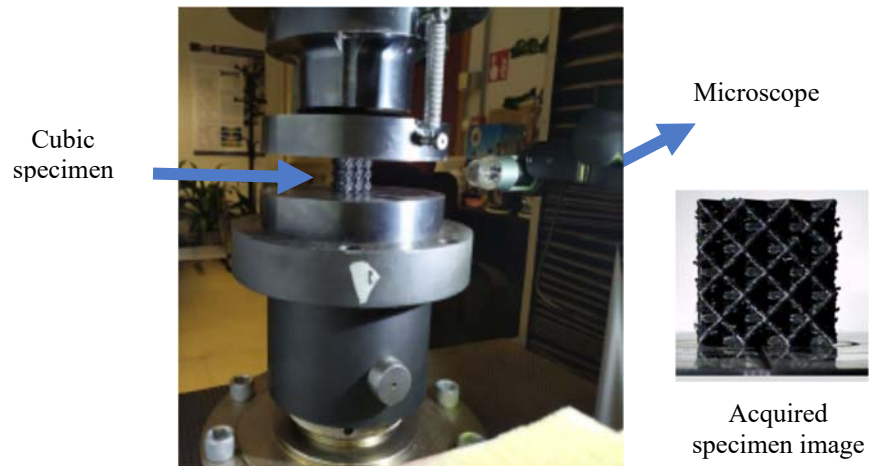
Fig. 3. Compression tests: testing setup and specimen image acquired with the microscope.

3. Compression tests on Carbon Nylon and on AlSi10Mg specimens

In this Section, the experimental results of the compression tests on carbon nylon specimens (Section 3.1) and on AlSi10Mg specimens (Section 3.2) are reported and analyzed.

3.1. Compression tests on carbon nylon specimens: experimental results

Fig. 4 shows the force-displacement curves for the five investigated cells (Fig. 1). For each cell geometry, two specimens are tested. Only one representative curve is shown in Fig. 4, since experimental scatter between two repetitions for each cell is limited.
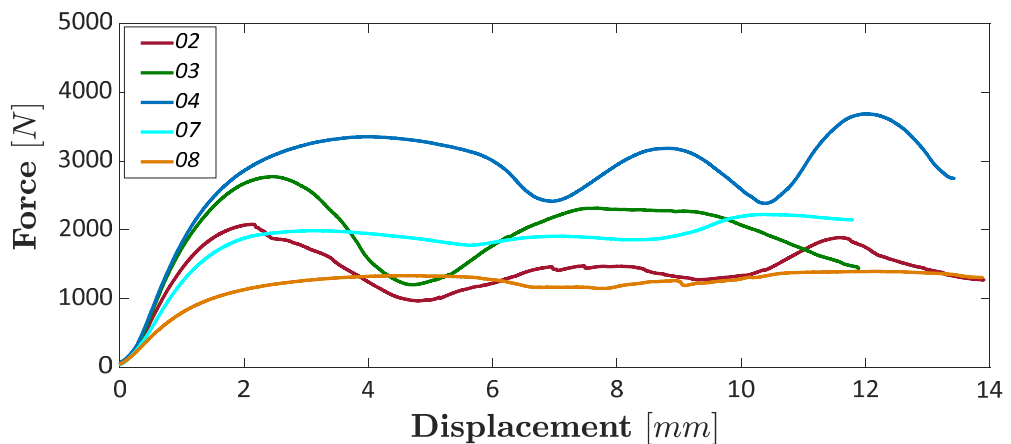

Fig. 4. Force-displacement curve for each cell geometry tested.

According to Fig. 4, the cell geometry strongly influences the compressive response, with very large differences. All the specimens show 3 peaks and 3 valleys in the plastic region. These peaks/valleys correspond to the failure of

one layer of cells. For the cell 08, this behaviour is less pronounced. The curve for the cell 04 is significantly above the other curves. For a proper comparison, the total absorbed energy and the specific energy absorption (SEA) parameter, i.e., the adsorbed energy per unit volume, have been compared. In particular, the SEA has been computed as the absorbed energy after the peak force divided by the compressed volume. In order to compute the compressed volume, the compressed length was multiplied by the average compressed area, obtained as the average area among 85 sections with steps of 0.1 mm. This parameter provides important indications on the energy-absorbing capabilities of each cell. Fig. 5 shows a bar plot of the absorbed energy and of the SEA in each compression test. In Fig. 5, the subscript "1t" refers to the first test, whereas the subscript "2t" refers to the second test.
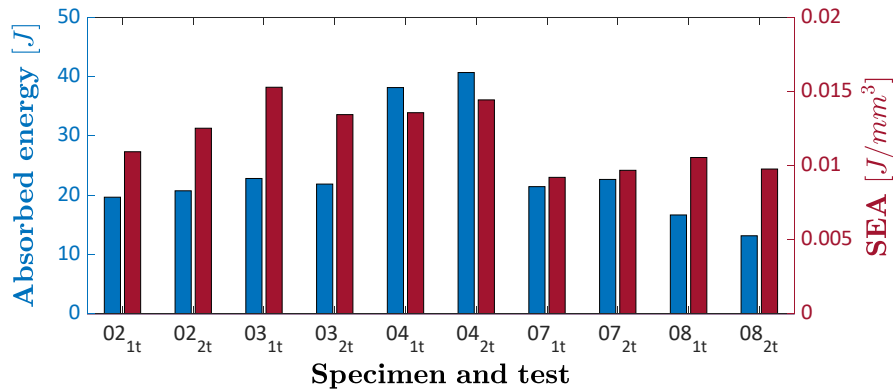

Fig. 5. Bar plot of the adsorbed energy and of the SEA for each compression test.

According to Fig. 5, the absorbed energy in cell 04 is the highest among all the investigated cells, as expected, being about twice the energy absorbed by other cells. The highest average SEAs, on the other end, are found for cell 03 and cell 04. Therefore, by considering the absorbed energy, the SEA and the force-displacement curve in Fig. 4, the cell 04 was selected as the cell with the highest absorbing capability.

3.2. Compression tests on the selected AlSi10Mg cell: experimental results

The cell selected in the analysis carried out in Section 3.1, cell 04, has been produced with an AlSi10Mg alloy through SLM and subjected to compression tests. Fig. 6 shows the acquired force-displacement curve for the AlSi10Mg specimens.
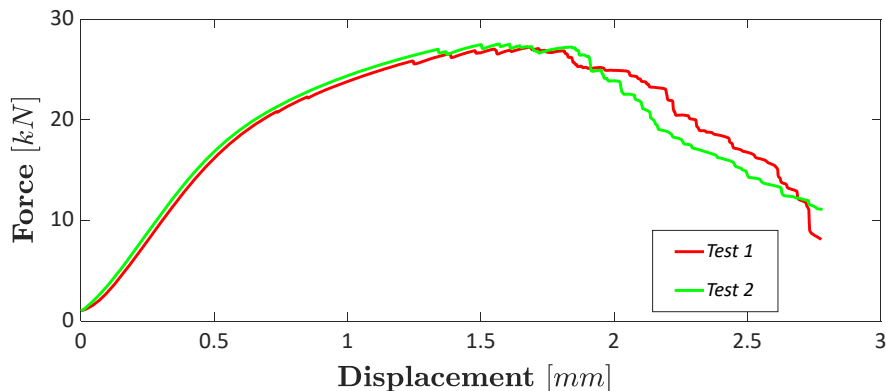

Fig. 6. Force displacement curves for the compression tests on AlSi10Mg specimens.

According to Fig. 6, the force-displacement curve shape is different from that found for the carbon nylon specimens and shown in Fig. 4. Indeed, the three peaks/valleys, corresponding to the layer failure, are not visible in Fig. 6, with the force dropping after the peak force, with a decrement larger than 60% of the peak force. The reason for this different behaviour is due to the different failure modes occurring with the AlSi10Mg alloy. Fig. 7 compares the failure modes of cell 04 made of carbon nylon (Fig. 7a) and of AlSi10Mg alloy (Fig. 7b).

Beginning of the compression

End of the compression

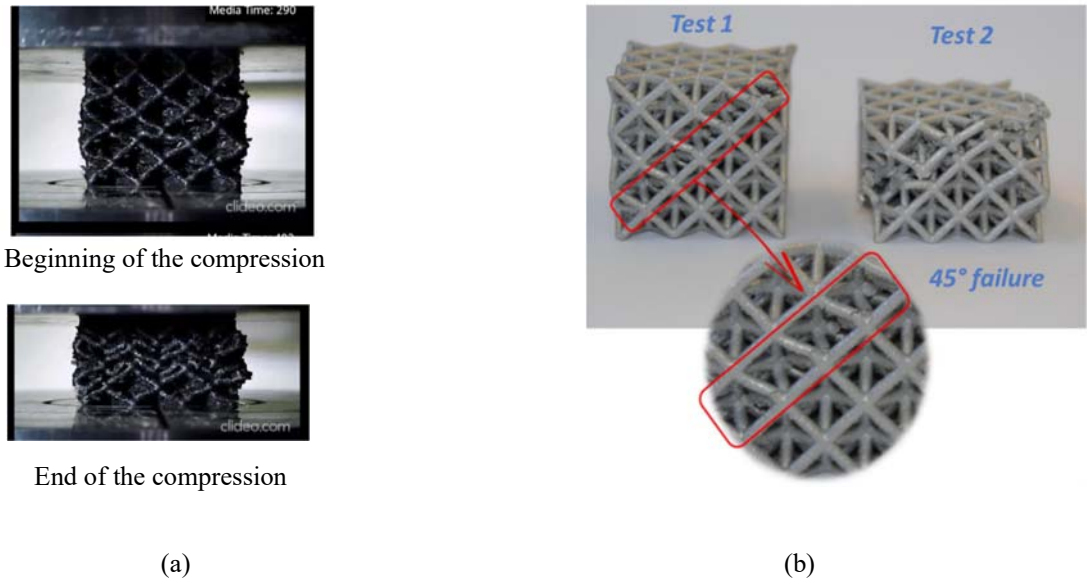(a)   (b)

Fig. 7. Comparison of the failure modes in compression tests; a) carbon nylon; b) AlSi10Mg specimens.

According to Fig. 7, the failure modes are different. Indeed, differently from the carbon nylon specimens, for which the three layers failed subsequently with high energy absorption, the AlSi10Mg specimens failed at 45° degree, with an abrupt decrement in the force-displacement curve. Even if the same specimens with the same cell are tested, the reason could be the different cell stiffness. This different behaviour after the peak force must be carefully taken into account when the cell response is simulated.

4. Simulation of the compression tests

In this Section the Finite Element Analyses (FEAs) carried out to simulate the compression tests are described. In particular, in Section 4.1 details on the specimen model are provided. In Section 4.2 and in Section 4.3, the model is validated on the experimental results obtained by testing the carbon nylon specimens and the AlSi10Mg specimens, respectively.

4.1. Specimen model

The compression tests are modeled by using the Altair suite. In particular, the specimen model is created by using the software Hypermesh, whereas the solver Radioss is used for the FEA simulation of the compression test. 1D beam elements are used for the specimen struts, in order to limit the simulation time. The experimental validation is therefore fundamental to prove that also a model with 1D elements can be effectively used to simulate the compression response of the investigated lattice structures.

The 1D beam elements, defined in Radioss according to the Timoshenko theory, have been connected to each other at the vertices. The properties of the beam elements are defined in a local coordinate system. Fig. 8 shows the specimen model, with applied loads and constraints.
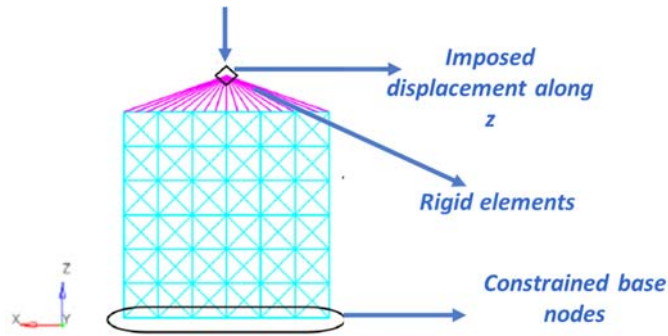
Fig. 8. Model of the specimen with 1D beam elements: applied loads and constraints.

According to Fig. 8, a uniform displacement on the upper face of the specimen is imposed by applying a displacement to a node located above the upper face and rigidly connected to all the nodes on the upper face. The node is forced to move along the z-axis and the degrees of freedom on x and y are locked. Finally, a constraint is applied to all the nodes at the base of the specimen to block the translation along the z-axis. The contact between the beam elements is modeled, during compression, with the "TYPE11" contact in Radioss.

Material properties are inserted in tabular form. In particular, the elastic range of the stress-strain curve of the material is modeled by using the elastic modulus and the Poisson's ratio that permit a proper fit of the experimental data. Instead, the real stress-strain curve is set point by point in the plastic region by digitizing the experimental curves reported in [14] for the caron nylon filament and in [15] for the AlSi10Mg alloy.

4.2. Carbon Nylon specimen FEA model: experimental validation

In Fig. 9 the FEA and experimental force-displacement curves are compared. The numerical curve is in agreement with the experimental curve. In particular, up to the peak force the two curves almost overlap. After the peak force, the FEA curve is close to the experimental curves. In particular, the numerical model is effective in modelling the failure of the first and of the third layer, with the two valleys occurring at the same displacement and with similar force decrements. On the other hand, in the FEA curve a net failure of the second layer is not evident. However, the difference between the absorbed energy (average experimental equal to 39.4 J and FEA equal to 38.7 J) is limited, proving the effectiveness of the model.

Moreover, by comparing the video recorded experimentally and the one obtained through the simulation, a similar failure mode is observed, with the lower layer failing first. This analysis confirms that a model with 1D elements can be exploited to accurately simulate the compressive response of lattice structures in a reasonable testing time, about ten minutes, with simulation results very close to the experimental ones.
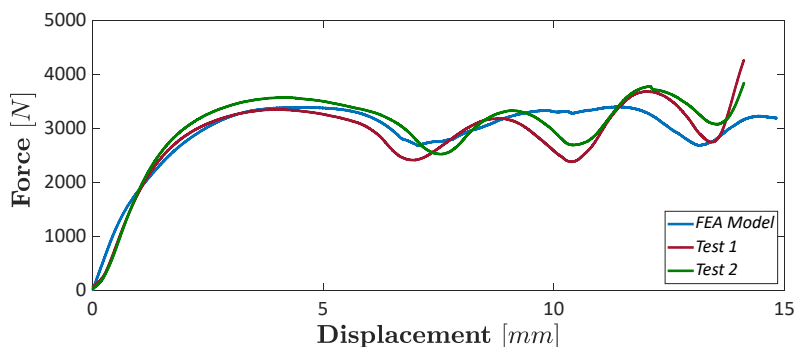

Fig. 9. Carbon Nylon lattice specimens: validation of the FEA model.

4.3. AlSi10Mg specimen FEA model: experimental validation

The FEA model developed for the simulation of the compression tests of carbon nylon specimens is used to simulate the compression tests of the AlSi10Mg alloy. However, it has been found that the model described in Section 4.2 does not permit to accurately simulate the mechanical response of the AlSi10Mg specimens: indeed, with the material properties considered for the carbon nylon specimens, the rapid drop of the force after the peak cannot be properly modeled. Therefore, a failure mode, called *failure plastic strain*, is added. With this failure mode, the plastic strain energy at which one 1D element fails can be defined: this value has been set by minimizing the difference between the experimental and the numerical curve. Fig. 10 compares the FEA and experimental force-displacement curves.
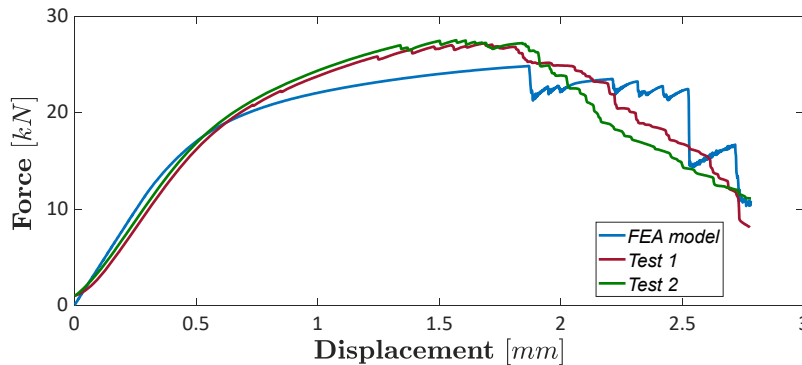

Fig. 10. AlSi10Mg lattice specimens: validation of the FEA model.

According to Fig. 10, the FEA model is in agreement with the experimental data. The difference in the elastic region is limited, whereas it increases if the peak force is considered. Moreover, with the introduction of the failure mode, the model is capable to simulate the failure mechanism of the AlSi10Mg cell, with the rapid force decrement after the peak force. It must be noted that, with this failure mode, the elements are deleted when the limit plastic strain energy is exceeded, thus justify the repeated abrupt drops of the force (vertical drops) in the numerical curve.

5. Conclusions

In this paper, the mechanical response under compression loads of specimens made of lattice structures was numerically and experimentally investigated. Compression tests on carbon nylon specimens produced through a fused deposition modeling process were carried out to assess the cell geometry ensuring the highest absorption capability, among the cells commonly adopted in the literature. In particular, five cell geometries were tested. Once the optimized cell has been selected, a finite element model of the selected cell has been created with the Hypermesh software. 1D beam elements have been used for the model, in order to limit the simulation time. The force-displacement curve obtained through simulation was found to be in good agreement with the experimental curve, with limited differences in the absorbed energy and with the simulated model capable to assess the experimental failure mode, characterized by gradual layer failures.

Compression tests were also carried out on AlSi10Mg specimens made with the optimized cell. For this material, a different failure mode was found, with a progressive failure of the struts at 45° degrees, that induces an abrupt decrement of the force after the peak. This test was also simulated by using the model developed for the carbon nylon specimens. However, for the AlSi10Mg specimens, additional material properties were introduced to properly model the experimental response. With these additional material properties, the experimental and the numerical curves were found to be in agreement, and the abrupt force decrement was properly simulated.

To conclude, the activity carried out in this paper showed that the mechanical response of lattice structures can be reliably simulated with 1D elements, in a limited testing time (about 10 minutes with respect to 80 hours for a model with 3D elements) and without loss of accuracy, as confirmed by the experimental validation. The model is effective

for materials with different properties and stiffness. However, the interactions between the cell stiffness, the base material and the failure mode should be experimentally verified to properly simulate the experimental response of lattice structures. These results provide useful indications for the design of components made of lattice structures and to be used in applications where energy absorption is required.

References

[1]   W.P. Syam, W. Jianwei, B. Zhao, I. Maskery, W. Elmadih, R. Leach, Design and analysis of strut-based lattice structures for vibration isolation, Precis. Eng. 52 (2018) 494–506. https://doi.org/10.1016/j.precisioneng.2017.09.010.

[2]   A. Seharing, A.H. Azman, S. Abdullah, A review on integration of lightweight gradient lattice structures in additive manufacturing parts, Adv. Mech. Eng. 12 (2020) 1–21. https://doi.org/10.1177/1687814020916951.

[3]   Y. Wang, S. Arabnejad, M. Tanzer, D. Pasini, Hip implant design with three-dimensional porous architecture of optimized graded density, J. Mech. Des. Trans. ASME. 140 (2018) 1–13. https://doi.org/10.1115/1.4041208.

[4]   I. Kaur, P. Singh, State-of-the-art in heat exchanger additive manufacturing, Int. J. Heat Mass Transf. 178 (2021) 121600. https://doi.org/10.1016/j.ijheatmasstransfer.2021.121600.

[5]   Z. Ozdemir, E. Hernandez-Nava, A. Tyas, J.A. Warren, S.D. Fay, R. Goodall, I. Todd, H. Askes, Energy absorption in lattice structures in dynamics: Experiments, Int. J. Impact Eng. 89 (2016) 49–61. https://doi.org/10.1016/j.ijimpeng.2015.10.007.

[6]   N. Jin, F. Wang, Y. Wang, B. Zhang, H. Cheng, H. Zhang, Failure and energy absorption characteristics of four lattice structures under dynamic loading, Mater. Des. 169 (2019) 107655. https://doi.org/10.1016/j.matdes.2019.107655.

[7]   G. Dong, Y. Tang, Y.F. Zhao, A survey of modeling of lattice structures fabricated by additive manufacturing, J. Mech. Des. Trans. ASME. 139 (2017) 1–13. https://doi.org/10.1115/1.4037305.

[8]   X. Cao, Y. Jiang, T. Zhao, P. Wang, Y. Wang, Z. Chen, Y. Li, D. Xiao, D. Fang, Compression experiment and numerical evaluation on mechanical responses of the lattice structures with stochastic geometric defects originated from additive-manufacturing, Compos. Part B Eng. 194 (2020) 108030. https://doi.org/10.1016/j.compositesb.2020.108030.

[9]   W. Chen, X. Zheng, S. Liu, Finite-element-mesh based method for modeling and optimization of lattice structures for additive manufacturing, Materials (Basel). 11 (2018). https://doi.org/10.3390/ma11112073.

[10]   F.N. Habib, P. Iovenitti, S.H. Masood, M. Nikzad, Fabrication of polymeric lattice structures for optimum energy absorption using Multi Jet Fusion technology, Mater. Des. 155 (2018) 86–98. https://doi.org/10.1016/j.matdes.2018.05.059.

[11]   A.I.H. Nasrullah, S.P. Santosa, T. Dirgantara, Design and optimization of crashworthy components based on lattice structure configuration, Structures. 26 (2020) 969–981. https://doi.org/10.1016/j.istruc.2020.05.001.

[12]   H. Lei, C. Li, J. Meng, H. Zhou, Y. Liu, X. Zhang, P. Wang, D. Fang, Evaluation of compressive properties of SLM-fabricated multi-layer lattice structures by experimental test and μ-CT-based finite element analysis, Mater. Des. 169 (2019) 107685. https://doi.org/10.1016/j.matdes.2019.107685.

[13]   Fabbrix NYLON CARBON 500 gr, (n.d.). https://www.crea3d.com/it/materiali-fabbrix/437-248-fabbrix-nylon-carbon-500-gr.html (accessed July 7, 2021).

[14]   F. Calignano, M. Lorusso, I. Roppolo, P. Minetola, Investigation of the mechanical properties of a carbon fibre-reinforced nylon filament for 3d printing, Machines. 8 (2020) 1–13. https://doi.org/10.3390/machines8030052.

[15]   A. Tridello, C.A. Biffi, J. Fiocchi, P. Bassani, G. Chiandussi, M. Rossetto, A. Tuissi, D.S. Paolino, VHCF response of as-built SLM AlSi10Mg specimens with large loaded volume, Fatigue Fract. Eng. Mater. Struct. 41 (2018) 1918–1928. https://doi.org/10.1111/ffe.12830.